Desalination and Water Treatment
www.deswater.com

doi: 10.5004/dwt.2018.23002

133 (2018) 268–282
November

Evaluating the use of measured and/or open access data in watershed modeling through an integrated modeling procedure

Stefanos Sevastas*, Ilias Siarkos, Nicolaos Theodossiou, Ioannis Ifadis

School of Civil Engineering, Aristotle University of Thessaloniki, GR54124 Thessaloniki, Greece, Tel. +30 2310326576; email: sevastas@civil.auth.gr (S. Sevastas), Tel. +30 2310661833; email: isiarkos@civil.auth.gr (I. Siarkos), Tel. +30 2310995660; email: niktheod@civil.auth.gr (N. Theodossiou), Tel. +30 2310995745; email: ifadis@civil.auth.gr (I. Ifadis)

Received 15 March 2018; Accepted 19 August 2018

ABSTRACT

Hydrological models are considered useful tools in both understanding and investigating the hydrological processes occurring on catchment-level. In order to develop hydrological models, various types of data are required, which, in many cases, are not available due to nonexistence of reliable measurements. To overcome measured data deficiency, open access data are often used. However, this can lead to faults in model development and, therefore, to inaccurate model results. In the study, the use of measured and/or open access data in watershed modeling is investigated and evaluated by developing three distinguished hydrological models for the Upper Anthemountas basin. To strengthen the whole procedure the hydrological models are coupled with a calibrated groundwater flow model, thus forming three separate integrated model systems. A key element of the procedure followed is the comparison between the new groundwater models and the calibrated one, leading to more reliable results regarding the use of measured and/or open access data. This procedure may be proven useful in researchers who desire to evaluate the use of various types of data, since it actually measures their influence through an integrated modeling procedure.

Keywords: Watershed modeling; Groundwater modeling; Surface water-groundwater interactions; Open access and measured data; Upper Anthemountas basin

1. Introduction

Water resources management requires the complete understanding of the various processes occurring on catchment-level, involving hydrological cycle, surface water, and groundwater flow, as well as surface water-groundwater interactions. Investigating the aforementioned processes is a complex procedure making water resources management rather demanding [1–3]. Hydrological models have proven to be useful and effective tools in the effort of supporting water management policy on catchment-level due to their ability to simulate and predict, both spatially and temporally, watershed response under various stresses. This is translated to the simulation of both hydrological processes (e.g., runoff, evapotranspiration (ET), and infiltration) and transport of sediments and nutrients taking into account the physical laws governing them [4–9]. Furthermore, hydrological models through their coupling with groundwater models significantly contribute to integrated water resources management, leading to the efficient and sustainable use of water [3,10,11].

Nevertheless, it is well-known that for the proper and accurate application of hydrological models the existence of a plurality of different types of data (i.e., data referring to the topography, land cover, soil types, and climate of the area under study) is required. In many cases, acquiring these data is not feasible since it could be a time-consuming and cost-intensive procedure, while it may be hindered due to accessibility constraints [4,12–14]. To overcome measured data deficiency in hydrological modeling, open access data are often used, thus allowing filling the gaps regarding vital missing

* Corresponding author.

Presented at the 6th International Conference on Environmental Management, Engineering, Planning and Economics (CEMEPE-2017), 25–30 June 2017, Thessaloniki, Greece

information; however, their credibility constitutes an issue of debate in literature [13,15–17].

More specifically, Fuka et al. [15] proved that reanalysis weather data are a reliable option for hydrologic simulations in a variety of hydroclimate regimes and basins in the USA. On the contrary, Roth and Lemann [16] indicated that the use of reanalysis weather data did not produce efficient discharge and sediment yield results in three small catchments in Africa. Jin et al. [17] specify that soil input data generated from field sampling soil analysis boosts hydrological modeling performance, whereas Boluwade and Madramootoo [18] argue that more accurate soil input does not necessarily increase the efficiency of hydrological simulations. In addition, Srinivasan et al. [13] concluded that an uncalibrated hydrological model based on accurate spatial input data can produce similar results regarding the hydrologic budget and sediment yield with a calibrated one in a basin in the USA. Overall, little can be found in literature about models that are built entirely using open access data series. Nevertheless, Rahman et al. [19] as well as Tan [20] concluded that hydrological models developed by applying a specific computer software, that is, the SWAT model, and using globally available free data can be successfully implemented providing satisfactory results.

In this perspective, the study investigates the use of measured and/or open access data in watershed modeling by comparing uncalibrated raw outputs in order to shed more light in this controversial issue. To achieve this task, three distinguished hydrological models were built based upon measured and/or open access data for the Upper Anthemountas basin, Halkidiki, Greece. Additionally, taking a step further from previous studies, the hydrological models developed herein were coupled with a calibrated groundwater flow model formed in the study as well, thus producing three different integrated model systems. The key point of the whole procedure is that the outputs of the hydrological models in terms of water percolation are introduced as inputs to the groundwater flow model, providing the aquifer recharge deriving from precipitation. In order to further investigate the effect of measured and open access data on modeling procedure, the results of the groundwater flow models in terms of hydraulic head distribution and aquifer water budget were also taken into consideration. What is worth mentioning is that in order to acquire a clear image of this effect, the results of the three new groundwater models were compared with the corresponding ones of the calibrated model, while the modification of various statistical errors used for testing model accuracy was taken into account as well.

For the development of the various hydrological models, the watershed loading/water quality model, Soil Water Assessment Tool (SWAT), in a GIS environment (ArcSWAT) was used. SWAT is a physically based, semidistributed model, operating on a continuous time scale with a daily time step. It is considered as one of the most complete models since it includes a large number of simulated components and can be used to predict the impact of land management practices on water, sediment, and agricultural chemical yield in a river basin scale over long periods of time [1,6,21]. A detailed description of SWAT is provided in Neitsch et al. [22] and Arnold et al. [23]. With regard to groundwater models, the MODFLOW code was applied. MODFLOW [24] is a modular, three-dimensional, finite-difference groundwater flow model which has evolved into the worldwide standard computer program used in groundwater modeling due to its ability to simulate flow in complex aquifer systems and its extensive publicly available documentation [25,26].

The aim of this study is to investigate to what extent the use of measured and/or open access data plays a significant role in hydrological modeling through the comparison and evaluation of the results of various integrated surface water-groundwater models. These results are associated not only with the results of hydrological models (i.e., hydrological cycle components) but also with those of groundwater flow models (i.e., hydraulic head, water budget, and model accuracy), thus strengthening the whole evaluation procedure and providing more reliable conclusions about the use of measured and/or open access data.

2. Materials and methods

2.1. Study area description

The Upper Anthemountas basin is located in the Chalkidiki peninsula, Greece, south-east of the city of Thessaloniki (Fig. 1) and constitutes the eastern part of the entire Anthemountas

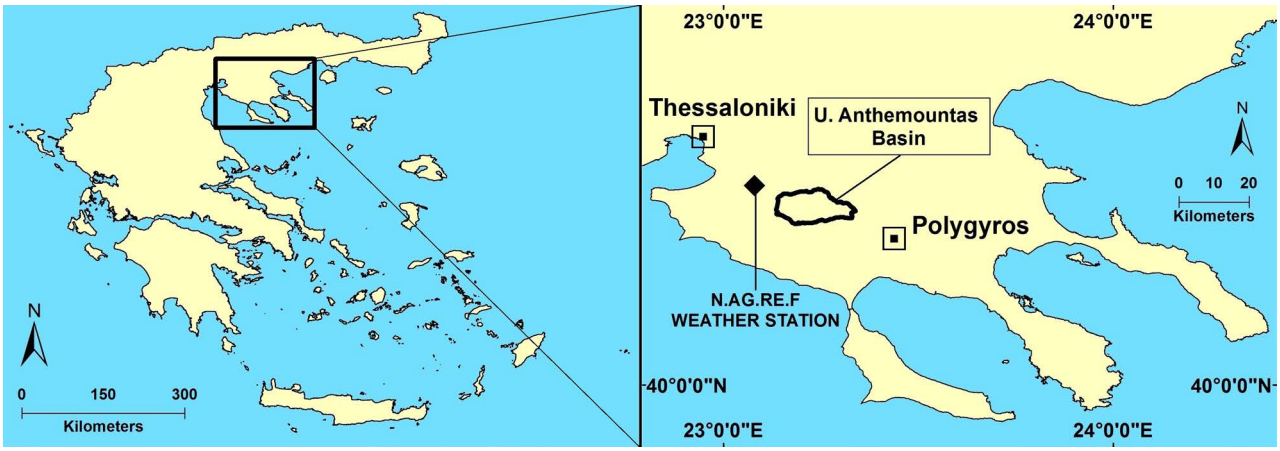

Fig. 1. Location of the Upper Anthemountas basin.

basin. The basin covers approximately 110 km^2, and it is bordered to the west by the Lower Anthemountas basin and to the south by the Moudania basin. Two major settlements, Galarinos and Galatista, and two minor, Ag. Anastasia and Kiourktsoglou, are sited within the catchment (Fig. 2) [5,27,28].

The Upper Anthemountas basin, which is a typical rural area, is dominated by complex cultivation patterns (wheat, corn, cotton, alfalfa, and olive trees) and mixed forest (mainly various types of oaks along with platanus and chestnuts trees). The geological structure of the area appears to be complex, combining a great variety of quaternary sediments (clays, sands, with intercalations of hard-grained material, quartzite pebbles, conglomerates, limestones, and sandstones), Neogene sediments (red clay series with marl, sand, and limestone lenses), along with various Mesozoic igneous and metamorphic fractured rocks (mainly epigneisses, greenschists, dunites, peridotites, and, secondarily, epidote-actinolite schists, two-mica gneiss, pyroxenites, gabbro, and diorites) (Fig. 3). In these formations, several aquifers – both porous and fissured rock aquifers – are developed composing a complex aquifer system in which both phreatic and semi-confined conditions exist according to the storativity value range (3.4×10^{-4}–6.2×10^{-2}) observed in the region [27,29–31]. Water from the whole aquifer system is extracted in order to meet various water needs and, therefore, wells in both porous and fissured rocked aquifers have been constructed (Fig. 2). Most of these wells are located in porous aquifers, which occupy the largest extent of the study area and are the most exploitable ones [27,30]. Water demand in the region is confined mainly to drinking and irrigation, and is met respectively through few public supply wells and a large number of privately owned irrigation wells, the latter due to the lack of an organized irrigation system. Moreover, there are few wells for both livestock and industrial purposes, as shown in Fig. 2 [5,27,28].

From hydrological point of view, the catchment consists of a dense well-formed stream network. Most time of the year, surface flow of the river is very limited due to relatively low precipitation and to the fact that some upper geological layers (i.e., Quaternary sediments) are mainly comprised of semipermeable soils (loams). As a result, the river appears to have surface outflows only for a short time after intense rainfall. Finally, the climate of Upper Anthemountas basin appears to be typically Mediterranean with relatively low annual precipitation (470 mm) and high temperatures during summer (Table 1) [5,27,28]. According to De Martonne Aridity index and Pinna Combinative index, the study area can be characterized as "Semi-Arid" and "Semi-Dry Mediterranean with formal Mediterranean vegetation," respectively [32,33].

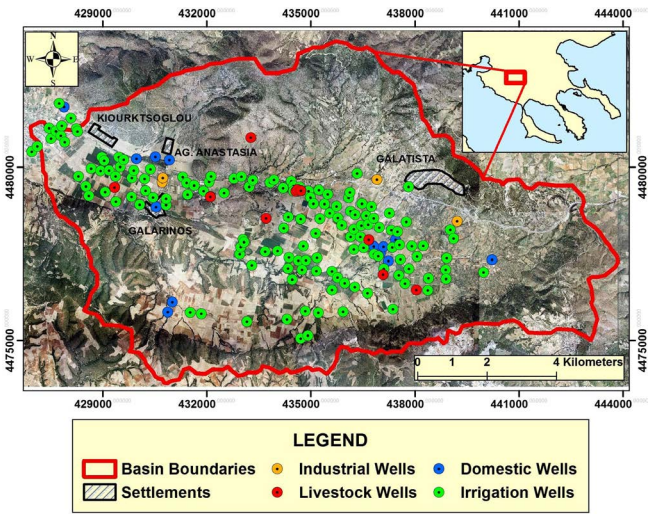

Fig. 2. Boundaries of the Upper Anthemountas basin, along with the settlements and the abstraction wells (per water use) sited within the basin.

2.2. Methodology

The procedure followed in the study aims to evaluate the use of measured and/or open access data in hydrological modeling, taking also into consideration the indirect impact of these data on groundwater flow regime through the aquifer recharge results deriving from the hydrological models. To achieve this task, the various hydrological models that were constructed using certain input datasets each time, were coupled with a calibrated groundwater flow model, thus forming several integrated surface water-groundwater model systems. Since SWAT was used for hydrological modeling, the aforementioned datasets are divided into four major categories: (1) climate data, (2) topography (elevation data), (3) soil, and (4) land use. More analytically, the procedure followed in this study includes the next steps (Fig. 4):

- Step 1 – Building three different hydrological models depending on which type of input data is derived from measurements or from open access datasets. These models are named as A, B, and C and are described in the following: (1) Model A – It is based exclusively upon public domain data and reanalysis weather data, (2) Model B – It is based predominantly upon measured data and climate data from a local weather station, and (3) Model C – It is built upon open access data, such as Model A, but with the same conventional climate data used in Model B.
- Step 2 – Building a steady-state groundwater flow model and coupling it with the hydrological models developed in Step 1. Their connection is established through the introduction of the hydrological models outputs, in terms of aquifer recharge, as inputs to the groundwater model.
- Step 3 – Running three separate groundwater flow simulations taking into account the different recharge values produced from the three different hydrological models (Step 1) and introduced into the groundwater model (Step 2). These models will be henceforth called GW Model A, GW Model B, and GW Model C according to the hydrological model they are based on.

3. Modeling procedure

3.1. Hydrological modeling

In the following, vital information about the various steps followed for acquiring the data used for the development of the three individual hydrological models is provided.

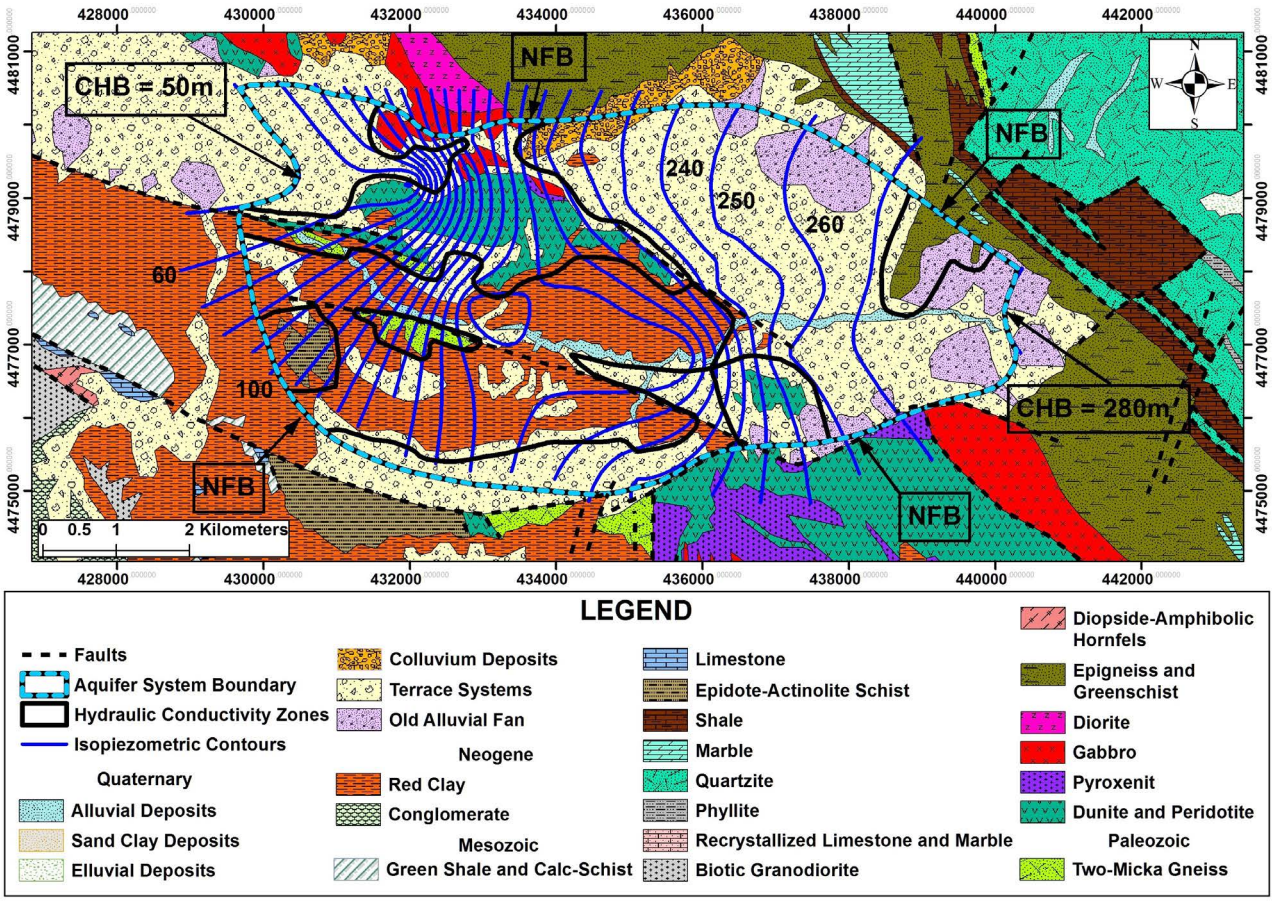

Fig. 3. Geological background of the study area (lithological units and faults were digitized from geological map sheets of the Institute of Geological and Mineral Exploration of Greece – I.G.M.E.), along with piezometric conditions (reference year 2000) and hydraulic conductivity zones.

Table 1
Weather data (mean temperature and mean rainfall) for Upper Anthemountas basin obtained from the National Agricultural Research Foundation (NAGREF) weather station

Years 1978–2016	Months												Mean annual
	Jan	Feb	Mar	Apr	May	Jun	Jul	Aug	Sep	Oct	Nov	Dec	
Mean Temp (°C)	5.3	6.6	9.6	13.9	19.1	24.3	26.6	26.0	21.6	16.2	10.7	6.4	15.5
Mean Rain (mm)	31.4	36.1	36.8	37.6	45.7	34.5	26.9	24.9	41.4	46.6	53.7	53.2	468.8

Model A

In Model A, a DEM map was produced by editing a 30 m (1 arc-second) resolution ASTER (Advanced Spaceborne Thermal Emission and Reflection Radiometer) GDEM (Global Digital Elevation Model) of the study area (tile N40E023) in ArcGIS, in order to delineate the watershed. Furthermore, the CORINE 2000 vector files, provided by the European Environment Agency, were collected in order to configure the land-cover of the basin. In addition, a 30 arc-second soil raster map, which contains all the basic spatial and attribute data concerning soil physical properties of the various soil types of the area, was extracted from the Harmonized World Soil Database (HWSD) [34] to be used as soil input in SWAT. Finally, the National Centers for Environmental Prediction's (NCEP) Climate Forecast System Reanalysis (CFSR) dataset was used as weather input data.

Model B

In this model, a topographic map was created by digitizing contours from 23 connected Hellenic Military Geographical Service (HMGS) map sheets, with a scale of 1:5,000 and 4 m contour line interval, which cover the entire basin. Then, the map was transformed into a Digital Elevation Model (DEM) in order to meticulously delineate the watershed.

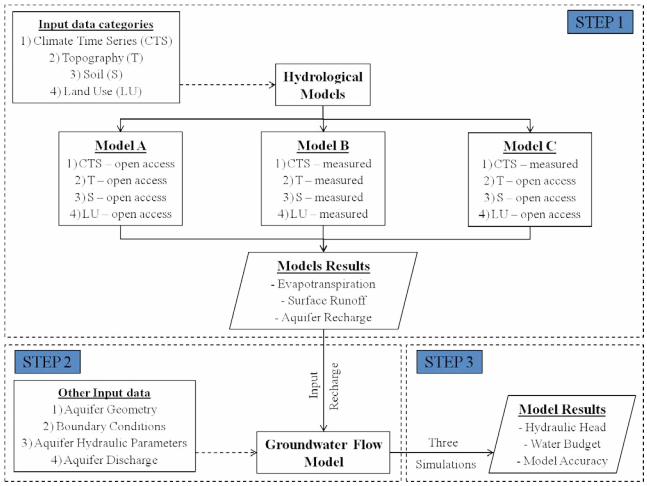

Fig. 4. Modeling procedure followed in the study.

The construction of a reliable spatial soil map and its corresponding attribute database was a rather challenging process, since no accurate soil data for the area under study existed. The procedure can be divided into two steps:

In the first step, an initial soil map was created by collecting and analyzing thirty two soil samples from all over the study area, from shallow (0–30 cm) and, where possible, deeper depths (30–100 cm) (Fig. 5). More specifically, various laboratory analyses of the samples were carried out with the purpose of defining the physical characteristics of the soil types that dominate the study area. To this task, sieve analysis, at first, and then a sedimentation process, using a hydrometer, were applied so as to determine particle size distribution (proportions of rock fragments > 2 mm, sand < 2,000–50 μm, silt < 50–2 μm, and clay <2 μm). Soil classes were defined using the U.S. Department of Agriculture (USDA) soil textural triangle (Fig. 5) and organic matter content (%OM) were measured via Loss on Ignition (LOI) [35]. Organic carbon content was then calculated according to Eq. (1) proposed by Pribyl [36]:

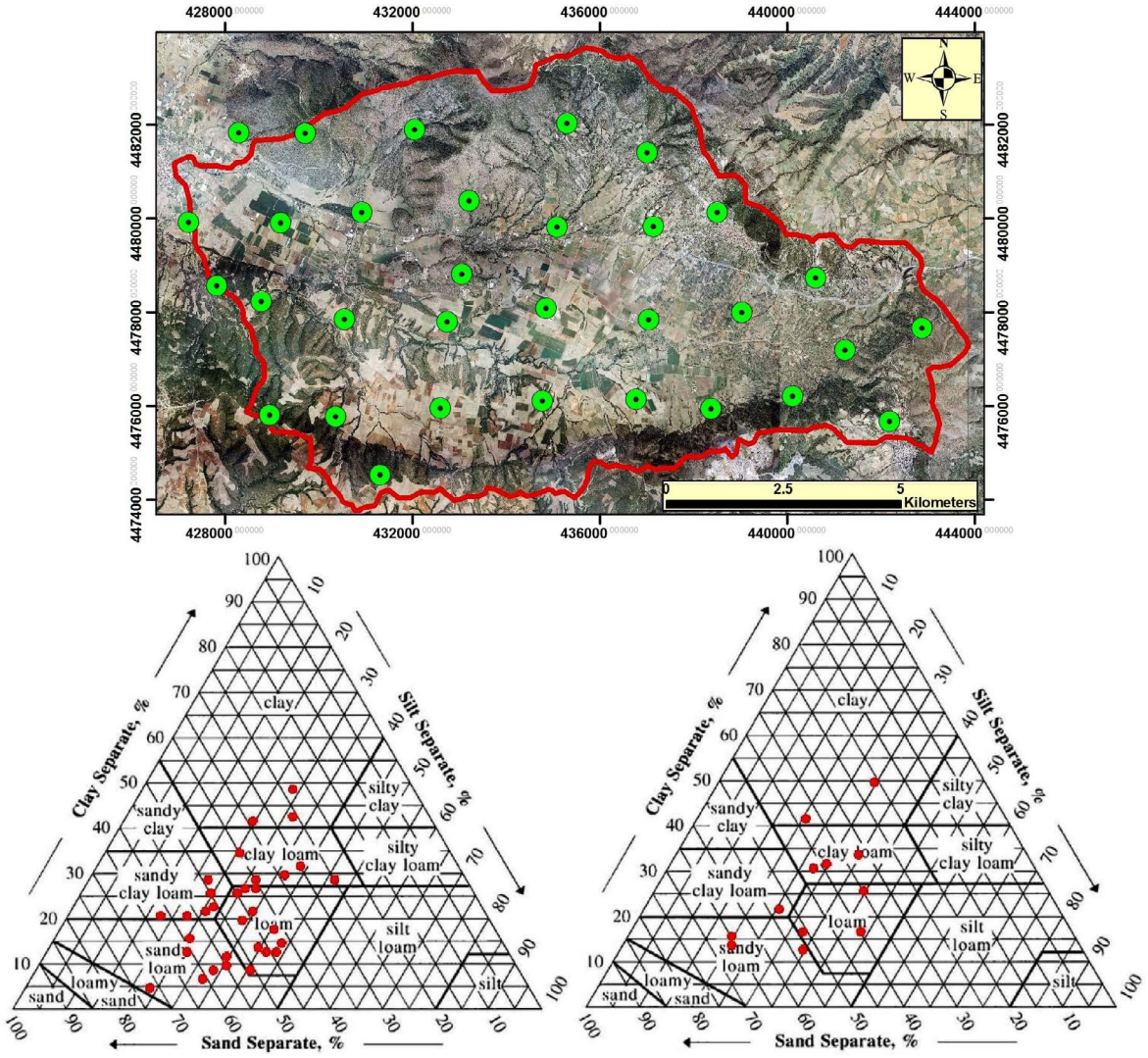

Fig. 5. Soil samples location and soil texture classes of shallow (lower left) and deeper (lower right) soil samples.

Organic matter (%) = Organic carbon (%) × 2 (1)

In-situ field measurements for saturated hydraulic conductivity were performed using a plain single ring technique proposed by Bagarello et al. [37], while soil albedo values were obtained from ten Berge [38]. Bulk density and available water capacity were calculated by applying the straightforward Soil Water Characteristic-Hydraulic Properties Calculator (SWC-HPC) Model, a graphic computer program developed by Saxton and Rawls [39], which has proven that can provide reliable results concerning various soil properties in the study area [29]. Moreover, the equations of Williams [40] were adopted to compute the erosion factor. Lastly, once all necessary soil parameters were defined, a soil map was created by generating Thiessen polygons in sample point sites.

In the second step, a separate "land capability" forestry map was retrieved from the School of Forestry and Natural Environment of the Aristotle University of Thessaloniki, containing information regarding the depth of the soils in the area. The final spatial soil map introduced to SWAT was the outcome of intersecting and editing the aforementioned maps.

Regarding land use, multiple field inspections were performed in the study area, during soil sampling period, so as to update the available CORINE 2000 land use map and, thus, acquire a more accurate land cover status of the basin.

Finally, in terms of climate input data, weather datasets from the National Agricultural Research Foundation (NAGREF) weather station were obtained, which is located 15 km away from the center of the basin. However, it should be noted that these datasets, consisting of precipitation and temperature values, were continuous on a daily step, thus applicable only for a period of 10 years (2002–2011).

Model C

Model C consists of the same input data as Model A, with the exception of using conventional meteorological data (NGREF dataset) instead of reanalysis data series.

For all hydrological models, the Hargreaves method was applied to calculate ET, due to limitations concerning the availability in meteorological data (daily data series of rainfall and temperature). An overview of all models developed in the study, as well as the data sources used for models development, are shown in Table 2. All input spatial layers, which are projected on the Greek Grid reference system, along with their attribute data imported to the models, are presented in Tables 3 and 4, as well as in Figs. 6 and 7. Furthermore, the outcomes of the watershed delineation for all models in addition to spatial information on the creation of hydrologic response units (HRUs), based on homogeneous soil, land use and slope characteristics, are given in Table 5 and Figs. 8 and 9. Lastly, descriptive statistics of local weather data (NGREF station) and reanalysis weather data series (CFSR dataset) are illustrated in Table 6.

3.2. Groundwater modeling

3.2.1. Conceptual model

A conceptual model is a realistic description of various characteristics of the reference area, as well as of the

Table 2
Overview of the models developed and data sources used for this study

Models	Input data source			
	Topography	Land cover	Soil	Climate
Model A	Aster GDEM	CORINE 2000	HWSD	CFSR dataset
Model B	HMGS map sheets	Updated CORINE 2000	Constructed soil map	NAGREF station
Model C	Aster GDEM	CORINE 2000	HWSD	NAGREF station

Table 3
Land cover of the study area and its reclassification according to SWAT database

CORINE description	SWAT land use database	SWAT code	Coverage (%)	
			Model A & C	Model B
Fallow land	Agricultural Land-Close-grown	AGRC	35	35
Complex cultivation patterns	Agricultural Land-Generic	AGRL	15	–
Permanently irrigated land	Agricultural Land-Row Crops	AGRR	–	8
Broad-leaved forest	Forest-deciduous	FRSD	8	–
Sclerophylous vegetation	Forest-mixed	FRST	33	50
Olive trees	Olive	OLIV	2	5
Pastures	Pasture	PAST	1	–
Transitional woodland/shrub	Range-brush	RNGB	2	–
Moors and heathland	Range-grasses	RNGE	1	–
Discontinuous urban fabric	Residential-Medium Density	URMD	2	2
Quarries				

Table 4
Soils in the study area

Models	Soil units	Description	Coverage (%)
Models A & C (from HWSD)	Fluvisols	–	7
	Vertisols	–	44
	Cambisols	–	49
Model B (constructed soil map)	SU1_MT	Shallow depth, medium texture soils (0–30 cm) (loams, sandy clay loams)	15
	SU1_CT	Shallow depth, coarse texture soils (0–30 cm) (sandy loams)	17
	SU2_MT	Medium depth, medium texture soils (0–60 cm) (loams, sandy clay loams)	7
	SU2_CT	Medium depth, coarse texture soils (0–60 cm) (sandy loams)	5
	SU3_FT	Deep, fine texture soils (0–100 cm) (clay, clay loams)	26
	SU3_CT	Deep, coarse texture soils (0–100 cm) (sandy loams)	9
	SU3_MT	Deep, medium texture soils (0–100 cm) (loams, sandy clay loams)	21

processes related to the problem under study. Building the conceptual model is the initial step of the groundwater modeling procedure, while it is considered an important part of it. This is due to the fact that the accuracy and reliability of the mathematical model significantly depend on the conceptualization procedure and the way the aquifer system is formed [28,41,42]. In the study, the conceptual model developed by Sevastas et al. [43] and improved in Sevastas et al. [28] was taken into consideration, while modifying it based on new geological and hydrogeological information gathered regarding the reference area for the needs of the study (e.g., Refs. [29,30,31,44–47]). In total, the key elements of the groundwater flow conceptual model are the following:

- The boundaries of the aquifer system (henceforth named as aquifer) (Fig. 3) include the whole set of loose formations located in the region, in conjunction with the rock formations of short extent, from which groundwater is also extracted, while excluding the rock formations surrounding the basin and being of limited water availability [28]. The inclusion of the fissured rocks in the aquifer system and their simulation in combination with the porous

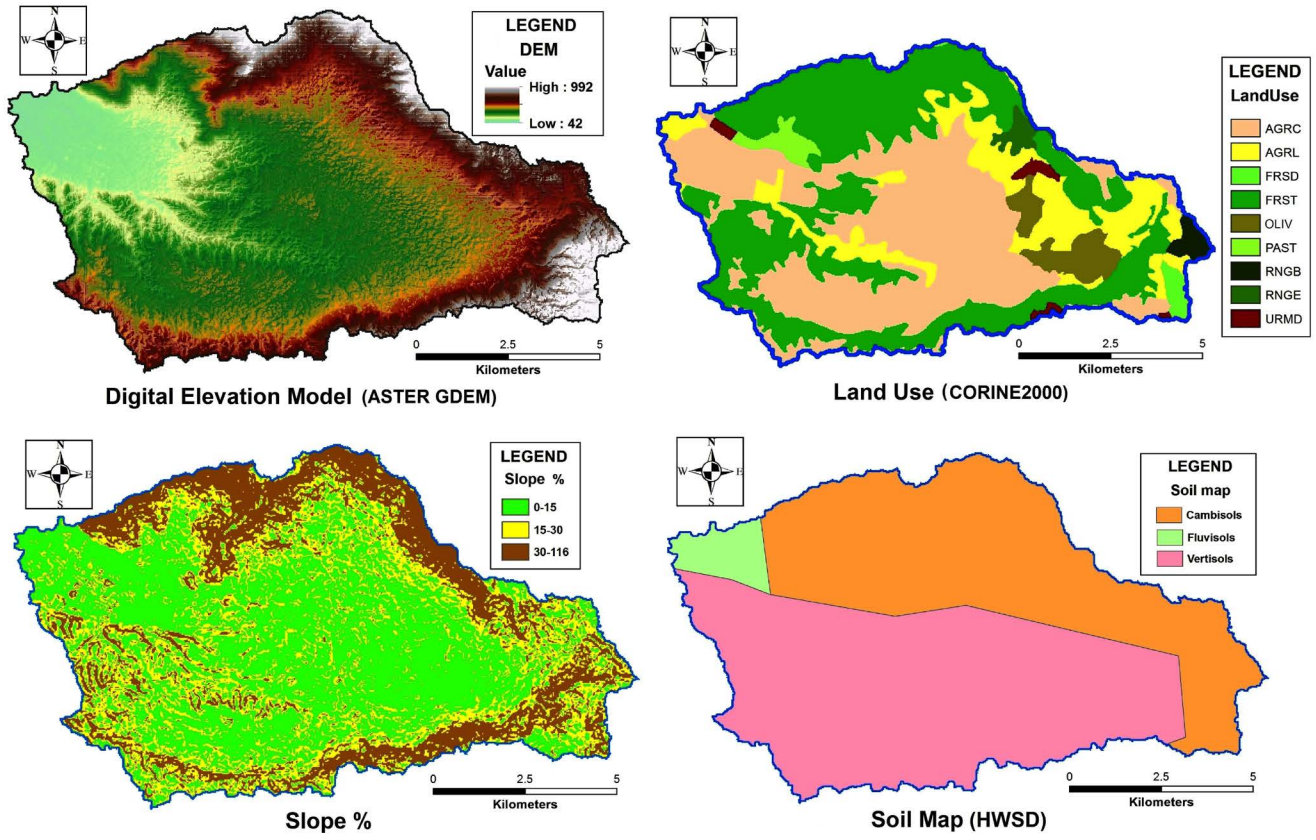

Fig. 6. Input data layers for Models A and C.

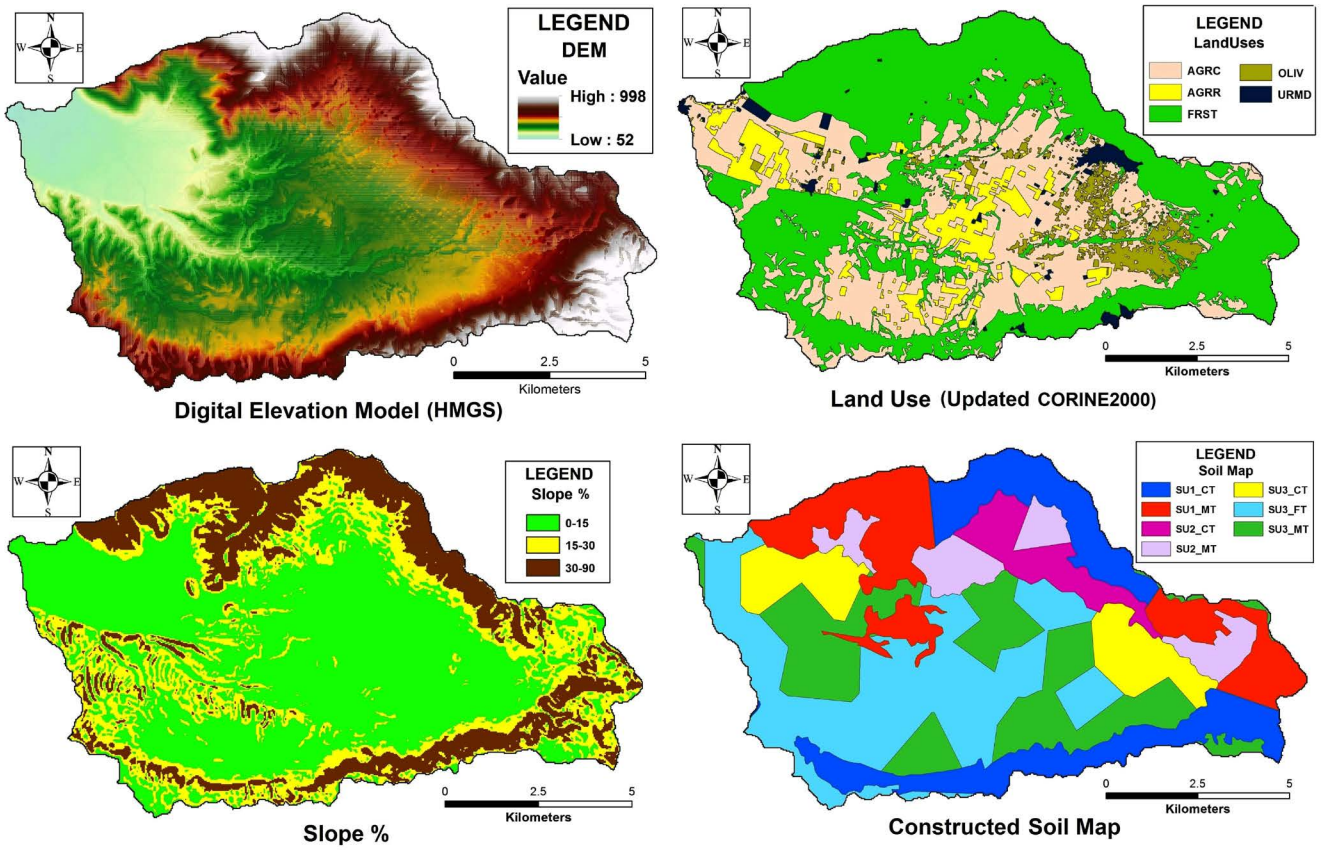

Fig. 7. Input data layers for Model B.

Table 5
Information on watershed delineation in Upper Anthemountas basin

Models	Basin area (km)	Sub-basins	Main reach length (km)	Total reach length (km)	HRUs
Models A and C	107.1551	23	20.663	49.756	289
Model B	106.4736	19	18.957	43.109	553

aquifers are based on the fact that fractured rocks are equivalent to a porous medium (EPM), in which structural discontinuities, cracks, raptures, and large faults can be treated as areas of higher hydraulic conductivity [48]. In addition, the method of EPM has been adopted in numerous studies and groundwater flow has been successfully simulated in fractured, weathered crystalline as well as karst aquifer systems, in various regions and climatic zones around the world (e.g., Refs. [49–53]).

- The aquifer's northern and southern boundaries were assigned as no-flow boundaries, since they were formed almost vertically to the isopiezometric contours (Fig. 3), which means that the direction of the groundwater flow is parallel to them [28,43]. The eastern and western boundaries were delineated as constant head boundaries with hydraulic head values set equal to 280 and 50 m, respectively [28,43], based on an isopiezometric map created by applying the Ordinary Kriging technique for the reference year 2000 (Fig. 3) [27].
- The whole aquifer system, including both the porous and the fissured rock aquifers, was considered of a uniform thickness of 180 m, based on a few available well logs referring to both types of aquifers.
- The aquifer's upper limit coincides with the ground level, while its lower limit is situated 180 m below the ground level taking into account the aquifer thickness assumed.
- Aquifer's hydraulic conductivity was determined based on the geology of the study area (Fig. 3) and, therefore, nine zones of hydraulic conductivity were considered (Fig. 10). In these zones, hydraulic conductivity values were derived from the respective literature, taking into account the type of geological formations existing in the region, due to the limited amount of pumping tests conducted in the study area. This literature includes both general literature (e.g., Refs. [54,55]) and various studies referring to the broader region of Thessaloniki and Chalkidiki peninsula (e.g., Refs. [44–47]). In particular, Veranis and Christidis [44] mention that water pressure

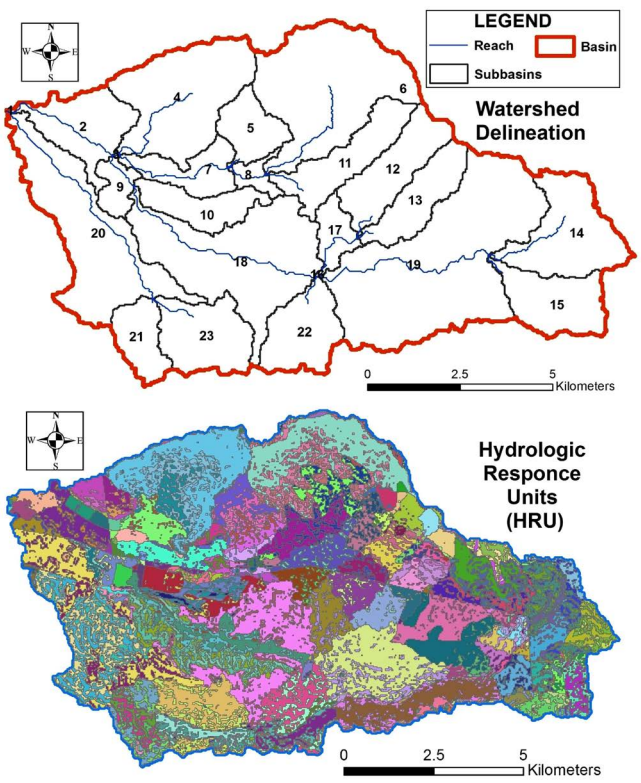

Fig. 8. Upper Anthemountas watershed delineation and HRUs created by SWAT (Models A and C).

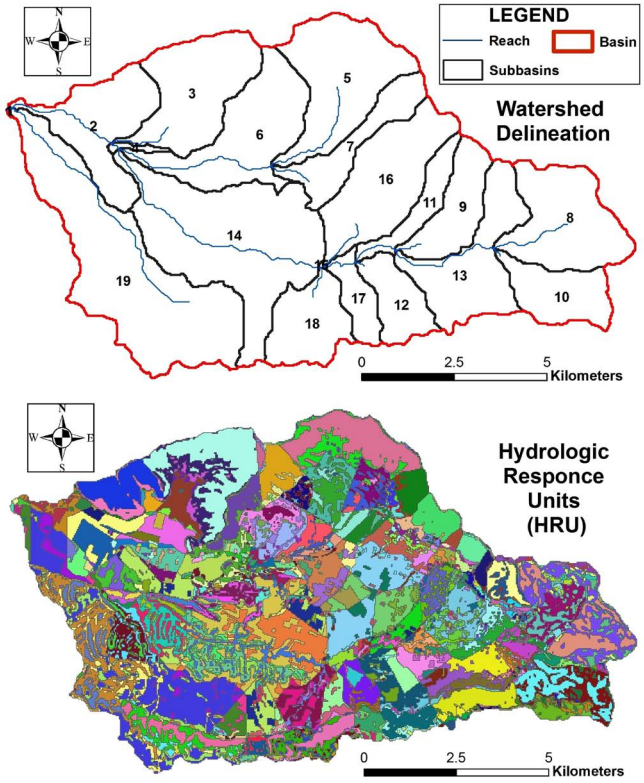

Fig. 9. Upper Anthemountas watershed delineation and HRUs created by SWAT (Model B).

Table 6
Descriptive statistics of local (NGREF) weather station and reanalysis weather (CFSR station) datasets, where min = minimum, max = maximum, aver = average, SD = standard deviation, and R^2 = coefficient of determination, between NGREF and CFSR values

Climate data	Units	NGREF station				CFSR station				R^2
		Min	Max	Aver	Sd	Min	Max	Aver	SD	
Rainfall	(mm)	0	91.6	1.6	5.1	0	157.2	2.4	6.8	0.39
Temperature (min)	(°C)	–11	23.8	9.8	7.2	–11.8	26.2	10.3	7	0.93
Temperature (max)		–2.3	44.3	21.4	9	–3.8	46.4	20.5	9.8	0.97

tests performed in boreholes in northeastern Chalkidiki area, reveal that hydraulic conductivity of weathered rocks (gneisses, phyllites, mica-schists, amphibolites, and serpentinites) has been estimated to vary from 10^{-9} to 10^{-4} m/s with a mean value of 10^{-7} m/s. Other measurements made exclusively upon gneisses show values from 7.1×10^{-7} to 2.3×10^{-6} m/s [45]. Furthermore, according to Stavri [46], the red clay series around the region of Thessaloniki have low conductivity values (10^{-7} to 10^{-6} m/s). However, much higher values (7.4×10^{-4} m/s) have been observed in certain locations [47]. On the other hand, based on few available pumping tests carried out in the study area, conductivity values for the quaternary sediments are considered in the range of 10^{-5} to 10^{-6} m/s [27].

- The aquifer is mainly recharged by rainfall and irrigation return flows (15% of irrigation water returns into the aquifer). Regarding the aquifer recharge from rainfall, three types of recharge zones were considered according to the geology of the study area, since the various geologic formations have a different effect on the recharge coefficient (Fig. 10). Specifically, the first zone consists of the quaternary sedimentary deposits, while the second one includes the outcrops of the fissured rocks and the third zone covers the red clay series of the Neogene. Finally, aquifer recharge was calculated on annual base using the simple form of the hydrological balance equation.
- The groundwater is abstracted through numerous abstraction wells (Fig. 2) in order to meet irrigation, domestic, livestock, and industrial needs. The pumping rates of these wells (i.e., equivalent pumping rate per water use) were estimated based on the total annual water consumption and the total number of operating wells per water use [28].
- Regarding the aquifer's eastern and western boundaries, their characterization as inflow or outflow boundaries is entirely based on model results and more exclusively on the aquifer's water budget.

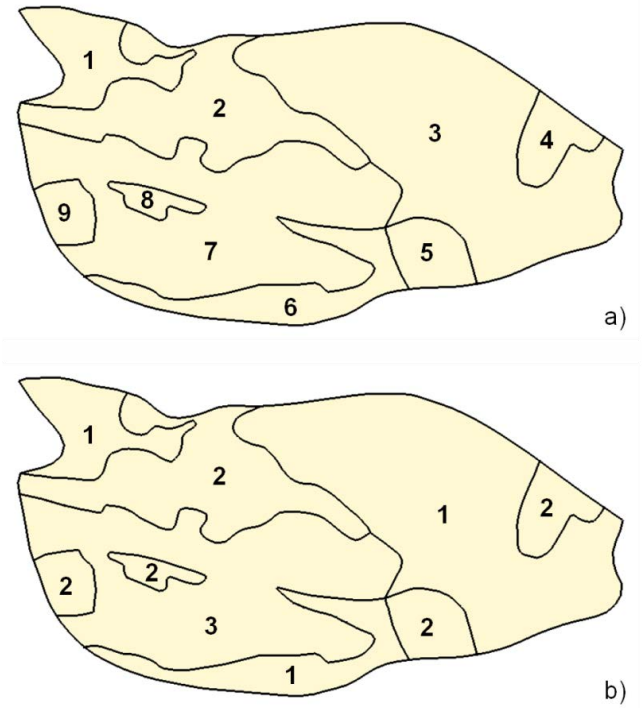

Fig. 10. (a) Hydraulic conductivity zones and (b) recharge zones, as both formed taking into account the geological background of the study area.

The aquifer conceptual model previously described was used in order to develop the steady-state groundwater flow model. The same conceptual model was also applied in the case of coupling between hydrological models and the groundwater model, making only one modification associated with aquifer recharge deriving from rainfall. More specifically, it was calculated by applying the SWAT model, instead of using the simple form of the hydrological balance equation, thus resulting in different values based on the HRUs spatial distribution as it was determined by the various hydrological models (different values and different spatial distribution of recharge for each hydrological model due to the differentiation of input data). However, even in this case, recharge values assigned to various HRUs were calculated on annual base, due to the type of the groundwater flow model used in this study (see Section 3.2.2). Particularly, the mean value of the annual recharge values for the whole simulation period was calculated and finally assigned to the HRUs.

3.2.2. Steady-state model

The groundwater flow simulation procedure involved the development of a calibrated steady-state model. This model, which will be henceforth called "Calibrated GW Model," was created based on the conceptual model described in Section 3.1.1. Since a steady-state model was developed, no temporal discretization was required. Some other basic information about this model includes its spatial discretization and calibration. With regard to the former, the model involves a single layer model grid with equal-sized cells in the horizontal plane (100-m side), which is comprised of 120 columns, 65 rows, and 1 layer (resulting in a vertically integrated two-dimensional areal model consisting of one layer which is characterized as convertible, that is, either confined or unconfined depending on the elevation of the computed water table). Regarding the model calibration procedure, it was accomplished using 15 observation wells monitored during October 2000 [27] by applying the PEST tool [56]. During the calibration procedure, various model parameters, such as hydraulic conductivity, pumping rates of irrigation wells, and aquifer recharge, were properly adjusted and determined. Table 7 presents the results of the adjustment of all the aforementioned parameters.

As expected, variations in hydraulic conductivity values were observed after model calibration and parameter adjustment. In particular, conductivity values were estimated from 0.131 to 0.863 m/d for the quaternary sediments, from 0.023 to 0.1 m/d for the fractured rocks, while a value of 0.105 m/d was computed for the red clay series. All the earlier calculations appear to be realistic, based on the geologic formations they refer to and in total conjunction with the values mentioned in various studies conducted in the broader region. In accordance, much higher values of aquifer recharge estimates were produced by the model concerning the quaternary sediments (0.3 mm/d), contrary to those of fissured rocks and red clays (0.183 and 0.16 mm/d, respectively). That is also to be expected, since the porosity of the sediments is much higher

Table 7
Estimated values of the various aquifer parameters submitted to calibration

Hydraulic conductivity for each zone (m/d)								
HK_1	HK_2	HK_3	HK_4	HK_5	HK_6	HK_7	HK_8	HK_9
0.4759	0.023	0.1310	0.069	0.065	0.863	0.105	0.100	0.100
Recharge for each zone (mm/d)								
RCH_1			RCH_2			RCH_3		
0.300			0.183			0.160		
Pumping rates of irrigation wells (m^3/d)								
Q_{irr}								
57.00								

compared with the other formations, thus enabling water to percolate much easier.

Moreover, the model accuracy was tested by calculating various statistical errors, such as mean error (ME), mean absolute error (MAE), and root mean square error (RMSE). So, the ME, MAE, and RMSE estimates were equal to –0.115, 1.578, and 2.175 m, respectively, indicating a rather successful calibration and, therefore, a satisfactory simulation. Fig. 11 shows the results of the steady-state model calibration in a scattergram of observed versus simulated groundwater levels, along with the 95% confidence intervals.

The results of the simulation are expressed as water table contour maps together with mass water balances for the model domain. Fig. 12 depicts the hydraulic head distribution produced by the model (along with the location of the 15 observation wells used for model calibration), making obvious the gradual decline of groundwater levels as moving from the eastern aquifer boundary to the western, where the contours appear to be denser. This is attributed to: (1) the hydraulic head value assigned to the western aquifer boundary and (2) to the hydraulic conductivity value of the rock formations existing in this specific part of the region and affecting the groundwater flow regime (Fig. 3). Table 8 presents the flow budget of the aquifer system. As it is obvious, groundwater inflow to the system occurs exclusively from recharge, which is due to precipitation and irrigation return water, while the main source of groundwater outflow is groundwater abstraction (74.0%).

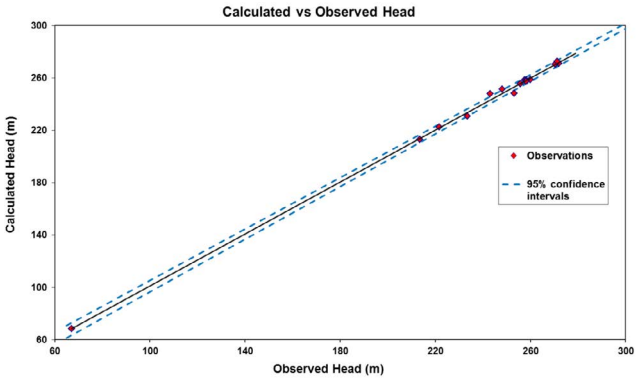

Fig. 11. Scattergram of observed versus simulated groundwater levels for the steady-state simulation.

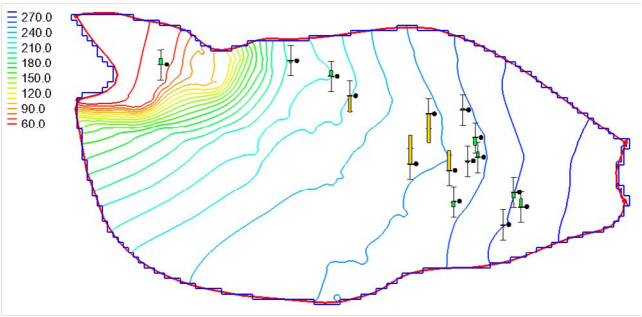

Fig. 12. Hydraulic head distribution according to the calibrated GW Model, along with the 15 observation wells used for model calibration.

Table 8
Aquifer flow budget for the calibrated GW model

	Inputs (m^3/d)	Outputs (m^3/d)	Inputs (%)	Outputs (%)
Constant heads	0.0	–2,647.6	0.0	26.0
Wells	0.0	–7,524.5	0.0	74.0
Recharge	10,172.1	0.0	100.0	0.0
Total source/sink	10,172.1	–10,172.1	100.0	100.0

The steady-state model described earlier was used in order to perform three separate simulations (groundwater Models A, B, and C) taking into consideration the results of the three individual hydrological models (Models A, B, and C) as far as aquifer recharge is concerned. In these simulations, all other parameters (i.e., boundary conditions, hydraulic conductivity, wells pumping rates, and irrigation return flows) remained constant and only recharge deriving from rainfall was modified based on hydrological models results. These results totally depend on the data used for building the hydrological models, thus making feasible the investigation of their indirect impact on groundwater model results. Finally, it should be mentioned that due to steady-state simulation conditions the mean value of the annual results deriving from hydrological models per HRU was used as input to the groundwater models.

4. Results and discussion

4.1. Hydrological modeling

All models were run for the same 10-year period, from 01/01/2002 to 31/12/2011, with a 2-year warm up in order to establish the initial conditions. Model outputs were obtained on a yearly step for 8 years (01/2004–12/2011) and are presented in Table 9.

The results deriving from all models display significant variations as shown in Table 9. First of all, rainfall from CFSR data series, used in Model A, is way overestimated. This immediately leads to severe inconsistencies in the water balance predictions, since SWAT model heavily relies on accurate rainfall data for modeling surface runoff and sediment loss [16].

Furthermore, major differences appear in aquifer recharge values among all models (Fig. 13). This can be

Table 9
Average annual water balance for Upper Anthemountas basin from 01/2004 to 12/2011

Parameters	Units	Model A	Model B	Model C
Rainfall	(mm)	861.2	524.1	
Surface runoff		20.61	8.13	7.93
Later flow		38.38	27.56	18.34
Aquifer recharge		401.02	86.64	123.40
Actual evapotranspiration		402.2	404.2	378.7
Potential evapotranspiration		986.7	1,177.2	
Total sediment loading	(kg/m^2)	0.075	0.007	0.026

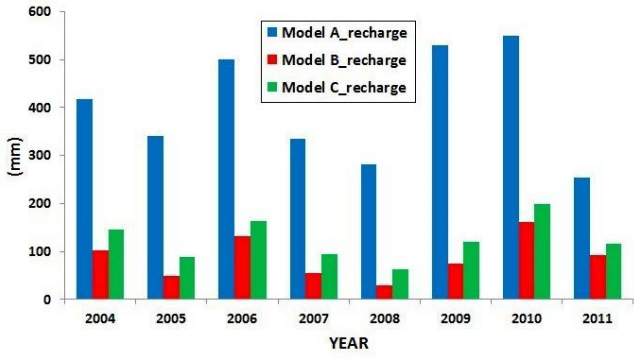

Fig. 13. Annual recharge values for Models A, B, and C for the 8-year simulation period.

attributed to: (1) low-resolution soil map and/or poor soil data provided by HWSD and (2) overestimated precipitation values introduced in Model A. Moreover, when comparing Models B and C, which use the same conventional weather data, aquifer recharge and lateral flow values, as part of the groundwater flow process, display significant disparities revealing the strong impact of accurate soil spatial and attribute data.

On the contrary, regarding potential evapotranspiration (PET), results from all models do not seem to diverge greatly. This could be due to the fact that the Hargreaves method, used for PET estimation, totally depends on temperature data, which show very good correlation between NGREF and CFSR stations (Table 6). Moreover, since actual ET predictions strongly rely on the land cover status of the area under study, it could be assumed that land use data do not seem to have a great impact on hydrologic simulations regarding the reference area.

Finally, in terms of sediment yield and surface runoff, poor values were generated from all models after simulation. However, this is consistent to the fact that for the greatest part of the year surface outflows in the basin emerge only for a short period of time and, notably, after intense rainfall events. Possible explanations for small discharge values can be attributed to the combination of many factors, which include: (1) Anthemountas basin belongs to the semiarid part of continental Greece with low annual rainfall due to rain-shadow effect [57], (2) semipermeable soils dominate the region, and (3) in general, relatively dense vegetation is observed in the study area.

4.2. Groundwater modeling

In this section, both the results of the three new groundwater models, in terms of aquifer water budget and models accuracy, and the results of the comparison between those three models and the calibrated one, in terms of hydraulic head distribution and aquifer recharge, are presented and discussed. First of all, Fig. 14 depicts the difference in hydraulic head distribution between the three new groundwater models and the calibrated one. As it is apparent, in the case of GW Model A, this difference is extremely high with a maximum value of 1,203.4 m and a mean value of 916.5 m (Table 10). It is reminded that GW Model A is based on hydrological

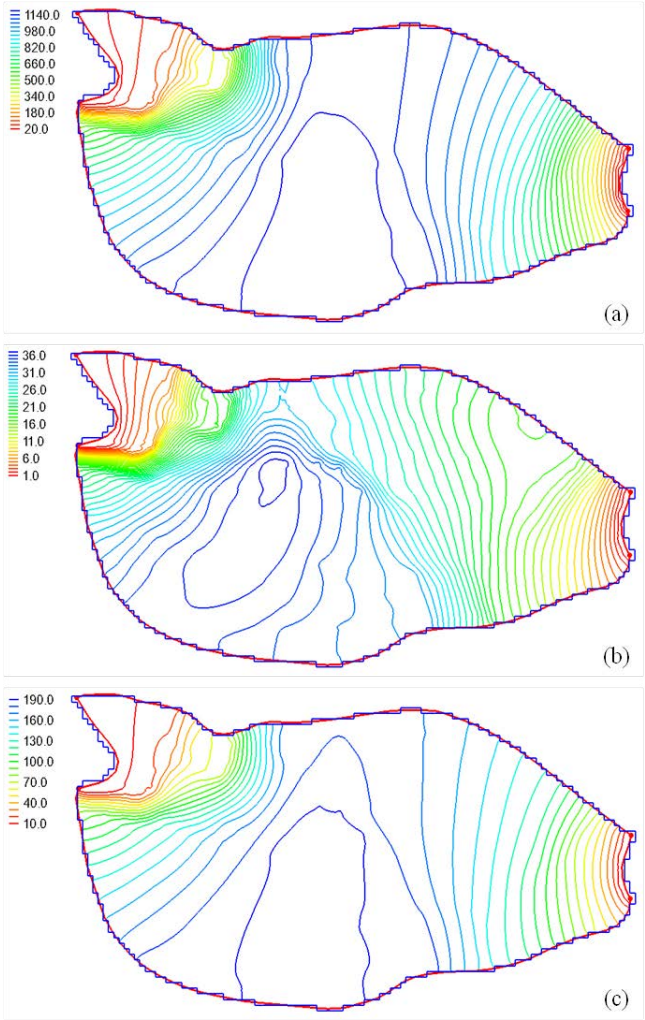

Fig. 14. Difference in hydraulic head distribution between (a) GW Model A – calibrated GW model, (b) GW Model B – calibrated GW model, and (c) GW Model C – calibrated GW model.

Model A, which is exclusively built upon open access data (public domain data and reanalysis weather data). On the contrary, the results of GW Model B appear to be closer to the corresponding ones of the calibrated model, since their difference has a maximum (absolute) value of 37.6 m and a mean (absolute) value of 25.1 m (Table 10). GW Model B is based on hydrological Model B for the development of which only measured data referring to the area under study were used. In Table 10 various statistical terms of all cases are presented.

Furthermore, Table 11 shows the flow budget of the aquifer system for all three new groundwater models, while Table 12 presents the difference in aquifer recharge between the new groundwater models and the calibrated one. In both cases, GW Model A provides the higher results, which is wholly attributed to the fact that the reanalysis weather data used for the development of hydrological Model A include high precipitation values. What is worth noting is that GW Model B, in comparison with the other two models, that is, GW Model A and GW Model C, results in recharge values closer to the calibrated GW model, while in all three models

Table 10
Several statistical terms regarding the difference in groundwater levels between the tree new models and the calibrated one

	Max (m)	Mean (m)	Median (m)
GW Model A – calibrated model	1,203.4	916.5	1,066.1
GW Model B – calibrated model	37.6	25.1	27.7
GW Model C – calibrated model	194.0	144.8	166.8

Table 11
Aquifer flow budget for the three new groundwater models

Models	Inputs		Outputs	
	Recharge (m^3/d)	Constant heads (m^3/d)	Wells (m^3/d)	Constant heads (m^3/d)
GW Model A	51,552.0	0.0	7,524.5	44,027.5
GW Model B	11,373.6	0.0	7,524.5	3,849.1
GW Model C	16,442.7	0.0	7,524.5	8,918.3

Table 12
Difference in aquifer recharge between the new groundwater models and the calibrated one

	Recharge (m^3/d)	Recharge (%)
GW Model A – calibrated GW model	41,379.9	406.8
GW Model B – calibrated GW model	1,201.5	11.8
GW Model C – calibrated GW model	6,270.6	61.6

aquifer recharge outcomes are higher than the corresponding ones of the calibrated GW model.

Finally, in Table 13 the values of various statistical errors for the new groundwater models are presented. According to these results, in all cases an increase of all statistical errors is observed in comparison with the errors of the calibrated model (see Section 3.2.2). This increase is lower in the case of GW Model B, which means that it approximates better the results of the calibrated GW model. As it was expected, according to the hydraulic head distribution (Fig. 14(a)), the higher values of statistical errors are observed in the case of GW Model A.

According to the analysis made earlier, it can be concluded that GW Model B provides better results (i.e., hydraulic head distribution, and aquifer water budget), since they appear to be closer to the corresponding ones of the calibrated model. Moreover, the model accuracy is less affected if the modified values of aquifer recharge produced by the hydrological Model B are imported to the groundwater model. All these conclusions reveal that both hydrological Model B and GW Model B, which are based exclusively on measured data, are able to approximate surface water and groundwater regimes in the reference area in a better way than the other models which are based (exclusively or partially) on open access data. Moreover, it should be mentioned that the aforementioned models can perform better if a rigorous calibration procedure and proper adjustment of aquifer recharge will be carried out.

Table 13
Statistical errors (ME, MAE, and MRSE) for the new groundwater models

	ME	MAE	MRSE
GW Model A	–941.925	941.925	974.543
GW Model B	–20.854	20.854	21.696
GW Model C	–144.341	144.341	149.122

5. Conclusions

In the study, the investigation and evaluation of the impact of the use of measured and/or open access data on watershed modeling were attempted, taking also into account the effect of these data on groundwater modeling. To achieve this task, three distinguished hydrological models were created for the Upper Anthemountas basin, which were coupled with a calibrated steady-state groundwater flow model, thus forming three integrated surface water-groundwater models. The data used for the development of the hydrological models (e.g., climate, elevation, soil, and land use data) involved measured data for the reference area, as well as open access data, such as reanalysis weather data and public domain data. Based on the available data, one model using exclusively open access data (Model A), one model using only measured data (Model B) and one model using both open access and measured data were built (Model C), which, in turn, resulted in three different groundwater models (GW Model A, GW Model B, and GW Model C).

Through the coupling between the hydrological and groundwater models, the evaluation of both the hydrological and groundwater models results was accomplished. Moreover, in the latter case, comparison of the results of the new groundwater models and the calibrated one also took place, which empowered the whole procedure providing more reliable conclusions about the influence of certain data on modeling procedure. With regard to the hydrological models, high variations especially on aquifer recharge results are observed, which leads to high variations on groundwater models results as well, since aquifer recharge is introduced to the groundwater models. More specifically, Model A provides extremely high values, which is wholly attributed to the high precipitation values of the reanalysis weather data. Model C follows while Model B resulted in the lowest recharge values.

Regarding the groundwater models, of particular interest is the results of the comparison between the new groundwater models and the calibrated one. Based on both hydraulic head distribution and aquifer water budget, GW Model B approximates better the calibrated model, since lower differences in the results than the other models are observed. Furthermore, the accuracy of GW Model B in terms of various statistical errors (ME, MAE and RMSE) is lower affected in comparison with the accuracy of the other two. This is considered to be rather essential since GW Model B is based on hydrological Model B which was developed using measured

data exclusively. Therefore, the aforementioned models are more representative for the area under study and require a few modifications through a rigorous calibration procedure in order to perform better.

In conclusion, it should be mentioned that extreme caution should be taken by researches who desire to develop hydrological models based, utterly, upon freely accessible input data, and especially in cases that no measured weather data are available. The procedure followed in the study may be proven useful in the effort of assessing the use of this type of data, since it actually measures their influence through an integrated modeling procedure.

Acknowledgments

An initial shorter version of the paper has been presented at the 6th International Conference on Environmental Management, Engineering, Planning, and Economics (CEMEPE) and SECOTOX Conference, Thessaloniki, Greece, June 25–30, 2017. All laboratory analyses of the soil samples were carried out in the Department of Geology of the Aristotle University of Thessaloniki, with kind permission from Professor V. Christaras and Assistant Professor N. Kantiranis. The authors would like to thank Assistant Professor M. Sapountzis of the School of Forestry & Natural Environment of the Aristotle University of Thessaloniki, for providing "land capability" forestry map of the study area. ASTER GDEM is a product of METI and NASA.

References

[1] B. Narsimlu, A.K. Gosain, B.R. Chahar, S.K. Singh, P.K. Srivastava, SWAT model calibration and uncertainty analysis for streamflow prediction in the Kunwari River Basin, India, using sequential uncertainty fitting, Environ. Process., 2 (2015) 79–95.
[2] M. Sophocleous, Interactions between groundwater and surface water: the state of the science, Hydrogeol. J., 10 (2002) 52–67.
[3] B. Wu, Y. Zheng, X. Wu, Y. Tian, F. Han, J. Liu, C. Zheng, Optimizing water resources management in large river basins with integrated surface water-groundwater modeling: a surrogate-based approach, Water Resour. Res., 51 (2015) 2153–2173.
[4] Z. Shen, Q. Huang, Q. Liao, L. Chen, R. Liu, H. Xie, Uncertainty in flow and water quality measurement data: a case study in the Daning River watershed in the Three Gorges Reservoir region, China, Desal. Wat. Treat., 51 (2013) 3995–4001.
[5] S. Sevastas, I. Siarkos, N. Theodossiou, I. Ifadis, K. Kaffas, Comparing hydrological models built upon open access and/or measured data in a GIS environment, Proceedings of the 6th International CEMEPE and SECOTOX Conference, Thessaloniki, Greece, June 25–30, 2017.
[6] M. Liu, J. Lu, Predicting the impact of management practices on river water quality using SWAT in an agricultural watershed, Desal. Wat. Treat., 54 (2015) 2396–2409.
[7] G.D. Gikas, T. Yiannakopoulou, V.A. Tsihrintzis, Modeling of non-point source pollution in a Mediterranean drainage basin, Environ. Model Assess., 11 (2006) 219–233.
[8] P. Santra, B.S. Das, Modeling runoff from an agricultural watershed of western catchment of Chilika lake through ArcSWAT, J. Hydro-Environ. Res., 7 (2013) 261–269.
[9] A. Fadil, H. Rhinane, A. Kaoukaya, Y. Kharchaf, O.A. Bachir, Hydrologic modeling of the Bouregreg watershed (Morocco) using GIS and SWAT model, JGIS, 3 (2011) 279–289.
[10] J. Cho, V.A. Barone, S. Mostaghimi, Simulation of land use impacts on groundwater levels and streamflow in a Virginia watershed, Agric. Water Manage., 96 (2009) 1–11.
[11] K. Spanoudaki, A. Nanou, A.I. Stamou, G. Christodoulou, T. Sparks, B. Bockelmann, R.A. Falconer, Integrated surface water-groundwater modelling, Global NEST, 7 (2005) 281–295.
[12] I. Siarkos, P. Latinopoulos, Modeling seawater intrusion in overexploited aquifers in the absence of sufficient data: application to the aquifer of Nea Moudania, northern Greece, Hydrogeol. J., 24 (2016) 2123–2141.
[13] R. Srinivasan, X. Zhang, J. Arnold, SWAT ungauged: hydrological budget and crop yield predictions in the Upper Mississippi River Basin, Trans. ASABE, 53 (2010) 1533–1546.
[14] M.A. Mekonnen, A. Worman, B. Dargahi, A. Gebeyehu, Hydrological modelling of Ethiopian catchments using limited data, Hydrol. Process., 23 (2009) 3401–3408.
[15] D.R. Fuka, M.T. Walter, C. MacAlister, A.T. Degaetano, T.S. Steenhuis, Z.M. Easton, Using the Climate Forecast System Reanalysis as weather input data for watershed models, Hydrol. Process., 28 (2014) 5613–5623.
[16] V. Roth, T. Lemann, Comparing CFSR and conventional weather data for discharge and soil loss modelling with SWAT in small catchments in the Ethiopian highlands, Hydrol. Earth Syst. Sci., 20 (2016) 921–934.
[17] X. Jin, L. Zhang, J. Gu, C. Zhao, J. Tian, C. He, Modelling the impacts of spatial heterogeneity in soil hydraulic properties on hydrological process in the upper reach of the Heihe River in the Qilian Mountains, Northwest China, Hydrol. Process., 29 (2015) 3318–3327.
[18] A. Boluwade, C. Madramootoo, Modeling the impacts of spatial heterogeneity in the castor watershed on runoff, sediment, and phosphorus loss using SWAT: I. Impact of spatial variability of soil properties, Water Air Soil Poll., 224 (2013) 1692.
[19] K. Rahman, N. Ray, G. Giuliani, C. Maringanti, C. George, A. Lehmann, Breaking walls towards fully open source hydrological modeling, Water Resour., 44 (2017) 23–30.
[20] M.L. Tan, Free internet datasets for streamflow modelling using SWAT in the Johor river basin, Malaysia, IOP Conf. Ser.: Earth Environ. Sci., 18 (2014) 012193.
[21] D.B. Othman, M. Gueddari, Hydrological study of the water quality of the Beja River according to the SWAT model, Desal. Wat. Treat., 52 (2014) 2047–2056.
[22] S.L. Neitsch, J.G. Arnold, J.R. Kiniry, J.R. Williams, Soil and Water Assessment Tool: Theoretical Documentation, Version 2009, Agricultural Research Service and Texas Agrilife Research, Temple, Texas, USA, 2009, p. 647.
[23] J.G. Arnold, R. Srinivasan, R.S. Muttiah, J.R. Williams, Large-area hydrologic modelling and assessment: part I. Model development, J. Am. Water Resour. Assoc., 34 (1998) 73–89.
[24] M.G. McDonald, A.W. Harbaugh, A modular three-dimensional finite-difference ground-water flow model, Techniques of Water Resources Investigations, Book 6, USGS, Reston, VA, 2009, p. 586.
[25] N.C. Ghosh, K.D. Sharma, Groundwater Modeling and Management, Capital Publications, New Delhi, 2006.
[26] M. Kouli, N. Lydakis-Simantiris, P. Soupios, GIS-based aquifer modeling and planning using integrated geoenvironmental and chemical approaches, L. Konig, J. Weiss, Eds., Groundwater: Modeling, Management and Contamination, Nova Science Publishers, New York, 2009, pp. 17–77.
[27] P. Latinopoulos, Investigation and exploitation of the water resources in the basin of Upper Anthemountas, Research Project, Final Report Prepared for: Municipality of Anthemountas, Aristotle University of Thessaloniki, Greece, 2001.
[28] S. Sevastas, I. Siarkos, N. Theodossiou, I. Ifadis, Establishing wellhead protection areas and managing point and non-point pollution sources to support groundwater protection in the aquifer of Upper Anthemountas, Greece, Water Utility J., 16 (2017) 81–95.
[29] S. Sevastas, D. Gasparatos, D. Botsis, I. Siarkos, K.I. Diamantaras, G. Bilas, Predicting bulk density using pedotransfer functions for soils in the Upper Anthemountas basin, Greece, Geoderma Reg., 14 (2018) e00169.
[30] N. Kazakis, K.S. Voudouris, Groundwater vulnerability and pollution risk assessment of porous aquifers to nitrate: modifying the DRASTIC method using quantitative parameters, J. Hydrol., 525 (2015) 13–25.

[31] N. Kazakis, G. Vargemezis, K.S. Voudouris, Estimation of hydraulic parameters in a complex porous aquifer system using geoelectrical methods, Sci. Total Environ., 550 (2016) 742–750.
[32] E. Baltas, Spatial distribution of climatic indices in northern Greece, Meteorol. Appl., 14 (2007) 69–78.
[33] I. Hrnjak, T. Lukić, M.B. Gavrilov, S.B. Marković, M. Unkašević, I. Tošić, Aridity in Vojvodina, Serbia, Theor. Appl. Climatol., 115 (2014) 323–332.
[34] FAO/IIASA/ISRIC/ISS-CAS/JRC, Harmonized World Soil Database (version 1.2), FAO, Rome, Italy and IIASA, Luxemburg, Austria, 2012.
[35] D.W. Nelson, L.E. Sommers, Total carbon, organic carbon, and organic matter, in: D.L Sparks, P.A. Helmke, A.L. Page, Eds., Methods of Soil Analysis - Part 3 Chemical Methods, Soil Science Society of America, Fitchburg, 1996, pp. 961–1010.
[36] D.W. Pribyl, A critical review of the conventional SOC to SOM conversion factor, Geoderma, 156 (2010) 75–83.
[37] V. Bagarello, S. Di Prima, M. Iovino, G. Provenzano, Estimating field-saturated soil hydraulic conductivity by a simplified Beerkan infiltration experiment, Hydrol. Process., 28 (2014) 1095–1103.
[38] H.F. ten Berge, Heat and water transfer in bare topsoil and the lower atmosphere, Pudoc Publications, Wageningen, 1996.
[39] K.E. Saxton, W.J. Rawls, Soil water characteristics estimates by texture and organic matter for hydrological solutions, Soil Sci. Soc. Am. J., 70 (2006) 1569–1577.
[40] J.R. Williams, The EPIC model, V.P. Singh, Ed., Computer Models of Watershed Hydrology, Water Resources Publications, Highlands Ranch, 1995, pp. 909–1000.
[41] J.J. Kaluarachchi, M.N Almasri, Conceptual model of fate and transport of nitrate in the extended Sumas-Blaine aquifer, Whatcom County, Washington, Project Report, Version 1.2, Utah State University, USA, 2002, p. 139.
[42] I. Ahmed, R. Umar, Groundwater flow modelling of Yamuna-Krishni interstream, a part of central Ganga Plain Uttar Pradesh, J. Earth Syst. Sci., 118 (2009) 507–523.
[43] S. Sevastas, I. Siarkos, N. Theodossiou, I. Ifadis, Simulating groundwater flow in the Upper Anthemountas basin in Chalkidiki applying MODFLOW and Geographic Information System, Proceedings of the 10th International Hydrogeological Congress, Thessaloniki, Greece, October 8–10, 2014.
[44] N. Veranis, C. Christidis, Hard rock aquifers of central and eastern Chalkidiki, region of central Macedonia, northern Greece, Proceedings of the 10th International Hydrogeological Congress, Thessaloniki, Greece, October 8–10, 2014.
[45] N. Veranis, C. Christidis, Hydrogeological conditions and groundwater qualities of the mountainous area of Krousia and Kerdyllia, Central Macedonia, N. Greece (in Greek), Proceedings of the 2nd Common Congress H.H.H.U. - H.C.M.H.R., Patras, Greece, October 11–13, 2012.
[46] E. Stavri, Settlements due to the excavation of twin tunnels of Thessaloniki Metro, section of New Railway Station - Agia Sofia (in Greek), MSc Thesis, National Technical University of Athens, Greece, 2013.
[47] A. Zevropoulou, Neotectonic faults of the wide area of Thessaloniki in association with foundation soils (in Greek), PhD Thesis, Aristotle University of Thessaloniki, Greece, 2010.
[48] B. Maihemuti, R. Ghasemizadeh, X. Yu, L. Padilla, A.N. Alshawabkeh, Simulation of regional karst aquifer system and assessment of groundwater resources in Manatí-Vega Baja, Puerto Rico, JWARP, 7 (2015) 909.
[49] M. Senthilkumar, L. Elango, Three-dimensional mathematical model to simulate groundwater flow in the lower Palar River basin, southern India, Hydrogeol. J., 12 (2004) 197–208.
[50] G. Panagopoulos, Application of MODFLOW for simulating groundwater flow in the Trifilia karst aquifer, Greece, Environ. Earth Sci., 67 (2012) 1877–1889.
[51] S.M. Yidana, Groundwater flow modeling and particle tracking for chemical transport in the southern Voltaian aquifers, Environ. Earth Sci., 63 (2011) 709–721.
[52] Z. Dokou, G.P. Karatzas, Saltwater intrusion estimation in a karstified coastal system using density-dependent modelling and comparison with the sharp-interface approach, Hydrolog. Sci. J., 57 (2012) 985–999.
[53] S.M. Yidana, D. Ophori, C.A. Alo, Hydrogeological characterization of a tropical crystalline aquifer system, J. Appl. Water Eng. Res., 2 (2014) 13–24.
[54] P.A. Domenico, F.W. Schwartz, Physical and chemical hydrogeology, 2nd ed., John Wiley & Sons, Inc., New York, 1998.
[55] B.B.S. Singhal, R.P. Gupta, Applied hydrogeology of fractured rocks, 2nd ed., Springer Science & Business Media, Dordrecht, 2010.
[56] J. Doherty, Manual for PEST, 5th ed., Watermark, Brisbane, 2002.
[57] D. Koutsoyiannis, N. Mamassis, A. Efstratiadis, N. Zarkadoulas, I. Markonis, Floods in Greece, Z.W. Kundzewicz, Ed., Changes of Flood Risk in Europe, IAHS Press, Wallingford, 2012, pp. 238–256.